View Article Online / Journal Homepage / Table of Contents for this issue

Anomalies in moisture transport during broccoli drying monitored by MRI?

Xin Jin,*[a] Antonius J. B. van Boxtel,[a] Edo Gerkema,[c] Frank J. Vergeldt,[c] Henk Van As,[c] Gerrit van Straten,[a] Remko M. Boom[b] and Ruud G. M. van der Sman[b]

Received 7th March 2012, Accepted 24th April 2012
DOI: 10.1039/c2fd20049j

Published on 24 April 2012. Downloaded by Michigan State University on 25/01/2016 03:40:31.

Magnetic resonance imaging (MRI) offers unique opportunities to monitor moisture transport during drying or heating of food, which can render unexpected insights. Here, we report about MRI observations made during the drying of broccoli stalks indicating anomalous drying behaviour. In fresh broccoli samples the moisture content in the core of the sample increases during drying, which conflicts with Fickian diffusion. We have put the hypothesis that this increase of moisture is due to the stress diffusion induced by the elastic impermeable skin. Pre-treatments that change skin and bulk elastic properties of broccoli show that our hypothesis of stress-diffusion is plausible.

1 Introduction

Magnetic resonance imaging (MRI) is an established technique for studying the internal states in biological systems. When coupled to in-situ thermal treatments MRI can be viewed as a rather novel enabling technology that yields unprecedented insights into the physical transport phenomena that occur during food processing.[1–6]

In this work, we apply MRI to investigate the changes in moisture distribution with time observed during *in-situ* drying of broccoli, which apparently violates Fick's law.

Convective drying of vegetables is mostly considered as a diffusion-controlled process.[7] Traditionally, in food science, diffusion is described by Fick's law, in which the mass flux is linear with the gradient in moisture content. A few papers in food science report deviations of moisture transport from Fick's law. Johnson *et al.* (1998)[8] reported an increased moisture content in the product centre during drying of plantain but without further explanation. Arnaud and Fohr (1988)[9] observed that the intra-kernel moisture content gradient increases during drying and decreases during tempering. Courtois *et al.* (2001)[10] and Toyoda (1988)[11] have considered the internal structure of products as a reason for deviation. In rice and corn there are internal regions with different moisture transport properties. Other deviations from Fick's law are reported for the cooking of starch-rich products, with moisture transport against the moisture gradient.[12,13] The deviations are said to be caused by gelatinization of starch during heating, which results in changes of local water holding capacity and water activity in the heterogeneous product. Different degrees of starch gelatinization result in different potential maximum moisture contents (ceiling moisture content). Therefore, the moisture transport during rice cooking

[a]*Systems and Control Group, Wageningen University, P.O. Box 17, 6700AA Wageningen, The Netherlands. E-mail: xin.jin@wur.nl; Tel: +31(0)317482014*
[b]*Food Process Engineering Group, Wageningen University, The Netherlands*
[c]*Laboratory for Biophysics, Wageningen University, The Netherlands*

View Article Online

Published on 24 April 2012. Downloaded by Michigan State University on 25/01/2016 03:40:31.

is driven by the difference of local moisture content and the ceiling moisture content. Watanabe *et al.* (2001)[14] proposed the so called "water demand" model to describe this transport phenomenon, which is not captured by Fick's law.

Furthermore, Wählby *et al.* (2001)[15] observed during experiments an increased moisture content in the product centre during the cooking of beef without clear explanation. Transport against the gradient in moisture content is thermodynamically possible if gradients in swelling pressure arise. Van der Sman (2007)[16] modelled swelling pressure-driven moisture transport (based on the Landau expansion of the Flory-Rehner theory) caused by protein denaturation near the product surface during the cooking of meat. In that model, the elasticity properties of the product play an important role and result in moisture transport in directions opposite to the moisture gradient. Recently, it has been shown that the full Flory-Rehner theory, indeed, holds for cooked meat.[17]

Another example is from the field of polymer physics where during drying the formation of a skin at the polymer surface resulted in water transport against the gradient in the moisture content. Okuzono and Doi (2008)[18] have called this phenomenon stress diffusion, and they formulated a generalized Fick's equation with an elastic term to describe the stress diffusion. In view of the preceding cited analysis and observations of non-Fickian moisture transport, we pose that the observed non-Fickian behaviour during broccoli drying is due to elastic stresses.

To test this hypothesis, we applied pre-treatments (blanching, freezing and peeling), which change the product structure and thus its textural and elastic properties. Experiments have been done in a MRI device with continuous and controlled *in-situ* hot air supply; the acquired MRI images provide data about moisture transport and shrinkage during drying. The different pre-treatments have been compared in terms of drying rates, shrinkage and moisture content profiles, *via* which the validity of our hypothesis is analysed.

2 Materials and methods

2.1 Materials

For all measurements, parts of the broccoli stalk were used. The sizes of the samples were about 0.01 m in height, 0.01 m in radius. Fig. 1 gives an example of a fresh broccoli sample.

2.2 Pre-treatments

In total six different pre-treatments were applied. An overview of the samples and pre-treatments is given in Table 1. After all pre-treatments, the free water at the sample surfaces was removed at room temperature with tissue paper.

Fig. 1 Cross section of a broccoli stalk sample.

 This journal is © The Royal Society of Chemistry 2012

View Article Online

Published on 24 April 2012. Downloaded by Michigan State University on 25/01/2016 03:40:31.

Table 1 Overview of pre-treatments and experiments

Pre-treatment	Procedure
Peeling	1.0 mm–1.5 mm of skin was removed
Blanching	90 °C water, 3 min
Freezing	−25 °C, 48 hours
Experiment	**pre-treatment**
1	Non treated
2	Peeled
3	Non-peeled, blanched
4	Peeled, blanched
5	Non-peeled, frozen
6	Peeled, frozen

2.3 Drying in the MRI device

The sample was fixed by a stick on a sample supporter and inserted into a drying chamber in the MRI measurement device. The size of the drying chamber was 0.032 m in diameter and 0.2 m in length. A continuous flow of temperature-controlled air was supplied. The air temperature was controlled at 30 °C or 50 °C, the air velocity at 1.0 m/s and the relative humidity at 10%.

Drying was continued until the moisture content of the samples was constant. Depending on the material properties, the experimental time for the fresh broccoli stalks ranged from 12 to 48 h. Initial and final product moisture contents (M_0, M_i) were determined by oven drying (105 °C, 24 h).

2.4 MRI imaging equipment

All measurements were performed on a 3 T (128 MHz for protons) MRI system (Bruker, Karlsruhe, Germany), consisting of an Avance console, a superconducting magnet with a 0.5 m vertical free bore (Magnex, Oxford, UK), a 1 T m^{-1} gradient coil, and a birdcage RF coil with an inner diameter of 0.04 m.

2.5 MRI imaging

3D images were obtained using a Turbo Spin Echo (TSE) MRI sequence,[19] a repetition time TR of 2 s, an effective spin echo time TE of 3.35 ms and a spectral bandwidth SW of 50 kHz. Only 16 echoes were acquired in the TSE train to avoid blurring due to T2-weighting. Odd and even echoes were separately phase-encoded forming two different images to avoid Nyquist ghost's artefacts, so the turbo factor was 8. Two acquisitions were averaged to improve image quality. The field-of-view (FOV) was 35 × 35 × 35 mm^3 with a matrix size of 64 × 64 × 64 resulting in a spatial resolution of 0.55 × 0.55 × 0.55 mm^3. The interval time between measurements was 34 min.

T2 mapping was done using a multi spin echo (MSE) imaging sequence,[20] a TR of 2 s, a TE of 3.59 ms and a SW of 50 kHz. Per echo train 128 echoes were acquired; 16 acquisitions were averaged to improve image quality. The FOV was 35 × 35 mm^2 with a matrix size of 64 × 64 resulting in an in-plane resolution of 0.55 × 0.55 mm^2. The slice thickness was 3 mm. The interval time between measurements was 34 min.

2.6 Numerical methods and data analysis

MRI-measurement data handling for graphical interpretation and analysis was performed with home-built software written in IDL (RSI, Boulder, CO). For shrinkage

View Article Online

Published on 24 April 2012. Downloaded by Michigan State University on 25/01/2016 03:40:31.

calculations, pixels with an intensity value above 0.75 (with the maximum value of 11.42 per pixel) were counted and for each pixel a volume of 0.16 mm^3 was assigned. By summing up the volume of all counted pixels the instantaneous volume (V_t) of the sample was calculated.

The degree of shrinkage is defined as the ratio of the reduced volumes ($V_0 - V_t$) to the initial volume (V_0):

$$S_V = \frac{V_0 - V_t}{V_0} \quad (1)$$

and the fraction of moisture removed from the initial product is:

$$S_m = \frac{M_0 - M_t}{M_0} \quad (2)$$

Where M_0, the initial moisture content, was measured by the oven method and M_t is the moisture content at different sampling time t.

2.7 MRI data calibration

For wet samples, the signal intensity is assumed to be linear with moisture content.[21] However, for nearly dry samples the intensity images are weak and deviate from the linear relationship. The minimum detectable liquid water concentration is about 20 kg m^{-3}.[22,23]

Hence, to establish the extent of linearity between MRI signal intensity and moisture content, we have plotted the shrinkage data as a function of the fraction of removed moisture. Assuming incompressibility of the solid and water present in broccoli, and the absence of air, the reduced volume must be attributed to the loss of moisture. In Fig. 2 we show this relation, which also indicates the accuracy of the interpretation of signal intensity to moisture content. It shows that below $S_m = 0.85$ shrinkage is more or less linear with the fraction of removed moisture, whereas in the last phase of drying ($S_m > 0.85$) there is a deviation from linearity. In this region, with product moisture content below 0.3 kg water kg^{-1} dry matter, the measured values might be lower than the actual values.

3 Results and discussions

3.1 Drying pattern of fresh broccoli stalks

Fig. 3 presents the MRI measurements for the central cross-section of fresh broccoli samples dried at 30 °C and 50 °C. Differences in brightness indicate the distribution of moisture throughout the sample; the brighter the colour, the higher the moisture content. The bar in the figures provides a relative scale for the moisture content. The gap at the bottom of each image indicates the hole made by the stick, which supports the sample. In the first image of both figures a slightly higher moisture content is observed at the edges. This indicates that there is still some free water at the surface, which is the consequence of cutting.

Fig. 3 shows an anomalous drying behaviour for both the 30 °C and 50 °C drying experiment for fresh and non-treated samples: after several hours of drying the moisture in the centre has been increased for the sample dried at 30 °C, the brightness at the centre of the images of row 2 is above that of row 1, and for 50 °C drying the brightness of the first image of row 2 is above that of the initial image.

Fig. 4 gives the intensity (proportional to moisture content) for the cross-section of the image at the start of drying and at 18.1 hours for drying at 30 °C, and at 6.8 hours for drying at 50 °C. We observe clearly that during drying, the moisture content in the centre rises far above the initial moisture content at any location of the sample. Compared to its initial value, the moisture content in the centre increases by 50–60%. This anomaly in drying behaviour evidently deviates from the standard

 This journal is © The Royal Society of Chemistry 2012

View Article Online

Published on 24 April 2012. Downloaded by Michigan State University on 25/01/2016 03:40:31.

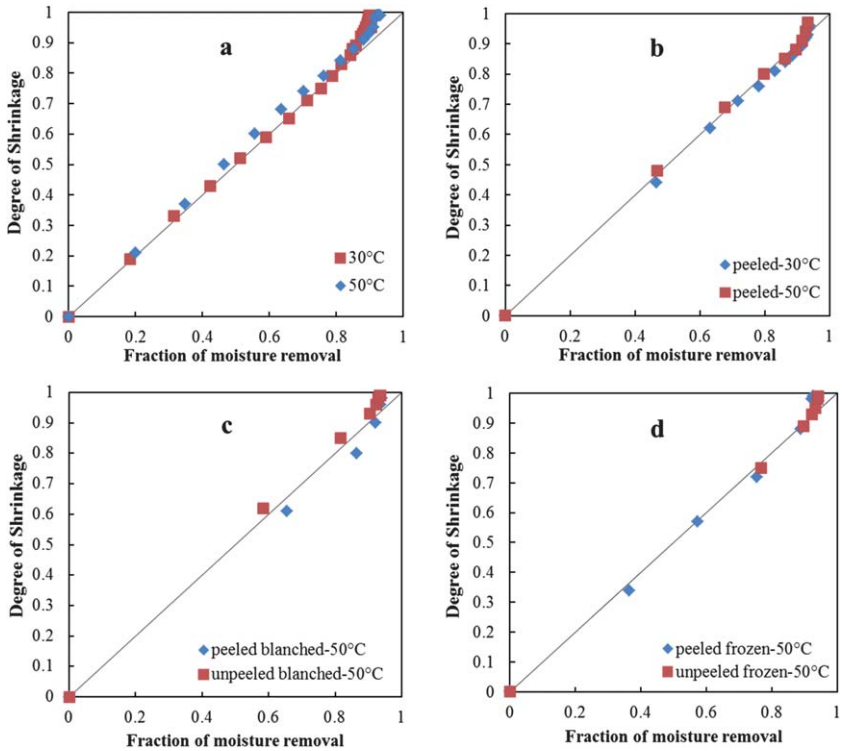

Fig. 2 Shrinkage as a function of the fraction of moisture removal. (a) unpeeled fresh samples at 30 and 50 °C drying, (b) peeled fresh samples at 30 and 50 °C drying, (c) peeled blanched samples and unpeeled blanched samples dried at 50 °C, and (d) peeled frozen samples and unpeeled frozen samples dried at 50 °C.

Fickian diffusion. According to the work of van der Sman (2007)[16] and Okuzono and Doi (2008),[18] shrinkage and deformation of the skin cause an internal pressure gradient, which results in a temporarily pressure-driven moisture transport towards the centre of the product.

Despite the increasing moisture content in the centre of the product, the drying curves for the full samples, which are given in Fig. 5, show monotonic decreasing moisture content.

Furthermore, the MRI images in Fig. 3 show the decreasing size of the samples due to shrinkage during drying. Fig. 2a shows the shrinkage quantitatively. The drawn lines in Fig. 2 correspond to the situation where shrinkage is equal to moisture removal. The data points for drying at 50 °C are above that for drying at 30 °C, which indicates that shrinkage at 50 °C is stronger than at 30 °C (Fig. 2a). This result can be explained by the relation of elasticity and moisture content. Krokida *et al.* (1998)[24] reported that in the high moisture content region, elasticity decreases with decreased moisture content, whereas in the low moisture content region, elasticity increases while moisture content decreases. During drying, the skin dries fast and due to the low moisture content the skin is more elastic and causes a centre-directed moisture transport.[16] Moreover, the skin forms a significant barrier for moisture transport and therefore moisture removal takes place in the longitudinal direction of the sample. It results in an early stage of drying in a "butterfly" shape.

The cross-sections in Fig. 4 also show that shrinkage differs for the height and width directions. For isotropic shrinkage of a cylindrical shape, the ratio (V_t/V_0) between the diameter at time t (d_t) and the initial diameter (d_0) is equal to the square

View Article Online

Published on 24 April 2012. Downloaded by Michigan State University on 25/01/2016 03:40:31.

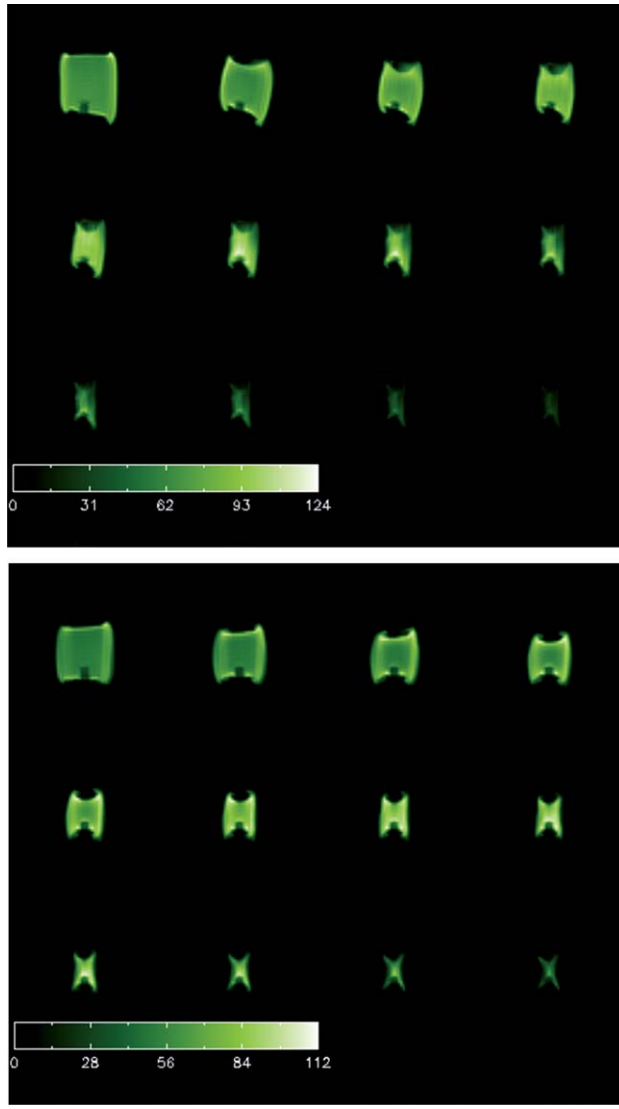

Fig. 3 Series of MRI intensity of the middle slice of fresh broccoli samples in time. Top: drying at 30 °C; time interval between samples 272 min, total time 50 h. Bottom: drying at 50 °C, time interval between samples 68 min, total time 12.5 h.

root of the volume ratio $(V_t/V_0)^{0.5}$ (with V_t the volume at time t, and V_0 the initial volume).

However, for the broccoli samples in Fig. 4, $(V_t/V_0) = 0.52$, while $(V_t/V_0)^{0.5} = 0.22$. The anisotropic shrinkage is caused by the impermeable and elastic structure of the skin and causes internal stress in the samples. From these results it is hypothesized that by applying pre-treatments that break down the wall structure the anomalies in drying behaviour could be reduced or even be cancelled.

3.2 Drying patterns after pre-treatments

To verify the hypothesis that the centre directed moisture transport is induced by the elastic properties of the product structure, product treatments were applied to break

 This journal is © The Royal Society of Chemistry 2012

View Article Online

Published on 24 April 2012. Downloaded by Michigan State University on 25/01/2016 03:40:31.

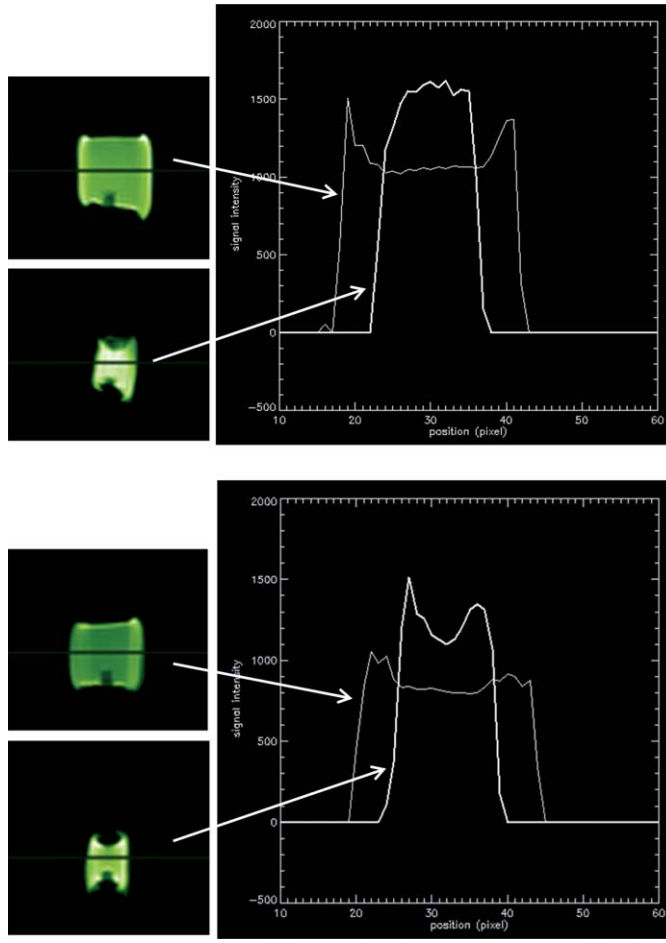

Fig. 4 MRI intensity values for a cross-section (given by the horizontal lines). Top: drying at 30 °C; initial sample and at 18.1 hours. Bottom: drying at 50 °C; initial sample and at 6.8 hours. In both cases, the moisture content in the centre of the samples surpasses the initial sample.

down the wall structure. The product treatments are (1) peeling: to remove the skin, (2) blanching: to soften the total tissue, both skin and core, thus to level out the elasticity differences between skin and center,[25] and (3) freezing and thawing: to break down the internal structure, and to change the elasticity of the internal structure.[5]

3.2.1 Peeling. The results for two drying temperatures are shown in the images of Fig. 6. Compared to Fig. 3, the increased moisture content hardly occurs, which confirms the role of elastic properties and the transport barrier of the skin. The first images also show increased moisture content at the surface, which is a result of moisture release at the surfaces where the skin was removed by cutting.

MRI images in Fig. 3 and Fig. 6 show different forms of shrinkage during drying. The peeled samples keep their original form for a long time, but towards the end of drying when the edge of the product approaches the glassy state, these samples also end with the "butterfly" shape. Fig. 2b presents the degree of shrinkage as a function of the fraction of removed moisture for the peeled samples at 30 and 50 °C. For a fraction of removed moisture below 0.85, shrinkage is linear to the fraction of removed moisture. For both temperatures the results coincide with the drawn line, which indicate the absence of an elasticity contribution to drying (see section 3.1).

View Article Online

Published on 24 April 2012. Downloaded by Michigan State University on 25/01/2016 03:40:31.

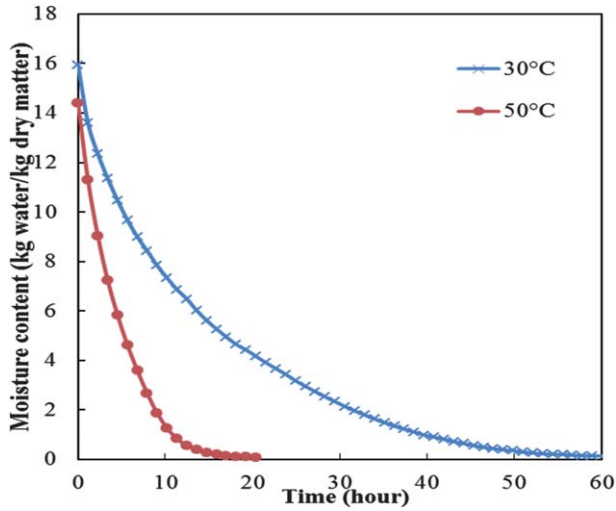

Fig. 5 Drying curves of fresh broccoli stalks at different drying temperatures (30 and 50 °C drying).

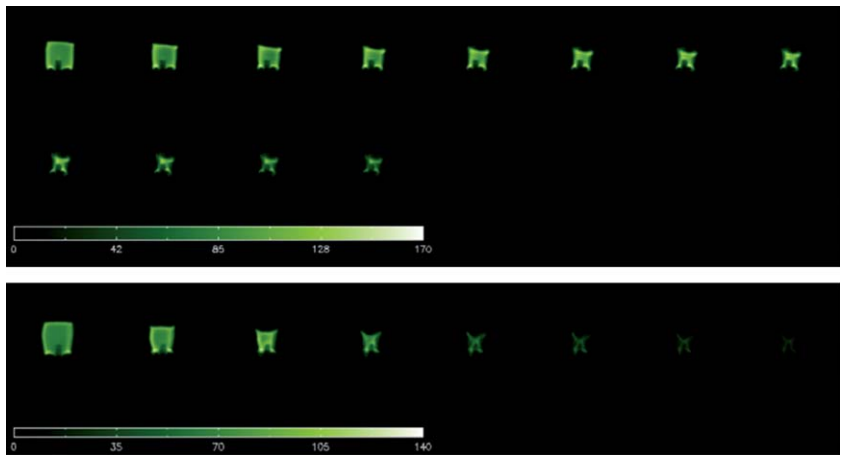

Fig. 6 MRI intensity of the middle slice of peeled broccoli stalks with respect to time. Top: drying at 30 °C; Bottom: drying at 50 °C. Total drying time, respectively, 12.5 and 9.0 h.

3.2.2 Blanching. Blanching results in tissue-softening and can level out the differences in mechanical properties between the core and the skin.[26] For the blanched samples only a small difference in drying behaviour between the peeled and unpeeled sample is found in Fig. 7. So, the barrier for mass transport by the skin is removed by only blanching. Not only the structure of the skin is softened, the internal matrix is also softened by blanching and, as a result, differences in elastic properties are levelled out, resulting in standard Fickian moisture transport. The drying time is reduced to about 4.5 hours. The drying rate of both samples is nearly equal, but the shrinkage of the peeled blanched sample is below that of the non-peeled sample (Fig. 2c).

3.2.3 Freezing. During freezing, ice crystals are formed in the tissue. Upon thawing, individual ice crystals merge into large complexes, which both break the structure and increase the internal pore size. With the destruction of internal structure,

 This journal is © The Royal Society of Chemistry 2012

View Article Online

Published on 24 April 2012. Downloaded by Michigan State University on 25/01/2016 03:40:31.

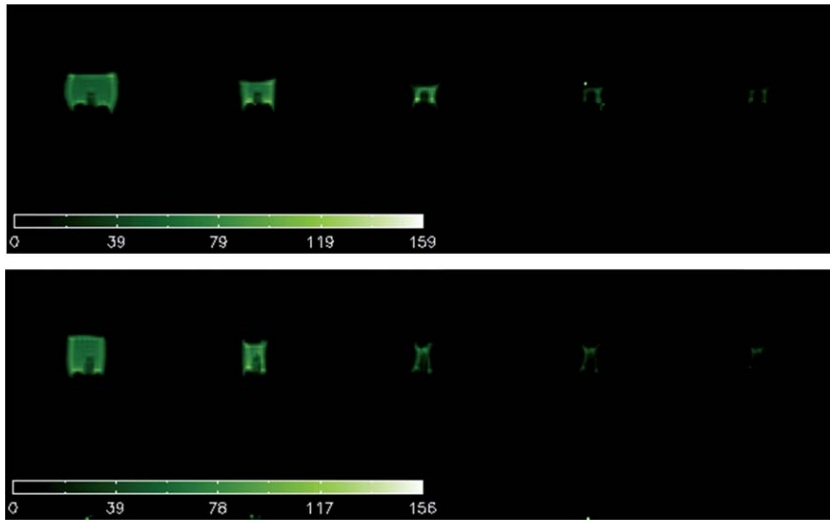

Fig. 7 MRI intensity of the middle slice of blanched broccoli stalks with respect to time. Samples are dried at 50 °C. Top: fresh unpeeled sample is blanched before drying. Bottom: sample first peeled then blanched before drying. Total drying time 4.5 hours.

elasticity is lowered. However, freezing is not effective enough to break down the barrier by skin. Results for peeled and non-peeled samples are given in Fig. 8. Due to the internal stress, the product shrinks easily during drying. The images in Fig. 8 show a strong "butterfly" form for the non-peeled frozen sample. The skin remains a mass transfer barrier. Drying occurs mainly along the longitudinal direction, and there is moisture accumulation just below the skin where the highest moisture content was detected.

The barrier for mass transport is absent for the peeled sample and therefore the peeled frozen sample does not have elastic stress-driven diffusion, and dries uniformly and the shape remains during drying and the moisture content in the centre decreases in time. For both samples, shrinkage was equal to the volume of lost moisture (see Fig. 2d). The change in the structure due to the freezing and thawing advances drying significantly and drying is completed within 4.5–5 hours.

4 Conclusions

From this investigation using in-situ MRI imaging of drying broccoli, and the above cited earlier reports, it is observed that moisture transport in foods can be due to moisture concentration gradients and gradients in elastic stress. In our case of pre-treated broccoli, the gradients in elastic stresses are probably induced by inhomogeneity in elastic properties of the skin compared to the core. During the drying of broccoli, the internal stress gradient can achieve a level that results in moisture transport against the gradients in moisture concentration. These observations are confirmed by pre-treatments that break down the internal structure and that of the product skin. Removing the skin of the broccoli sample by peeling results in a uniform product with drying behaviour close to Fickian diffusion. Blanching as a pre-treatment softens the skin and core of the product and creates uniform properties throughout the material to be dried. In this case drying can, indeed, be considered as a diffusion-driven process. Freezing and subsequently thawing as pre-treatment of fresh broccoli does not change the inhomogeneity of the elastic properties of the product during drying. In addition, we have observed that the pre-treatments peeling, blanching and freezing all enhance the drying rate significantly.

View Article Online

Published on 24 April 2012. Downloaded by Michigan State University on 25/01/2016 03:40:31.

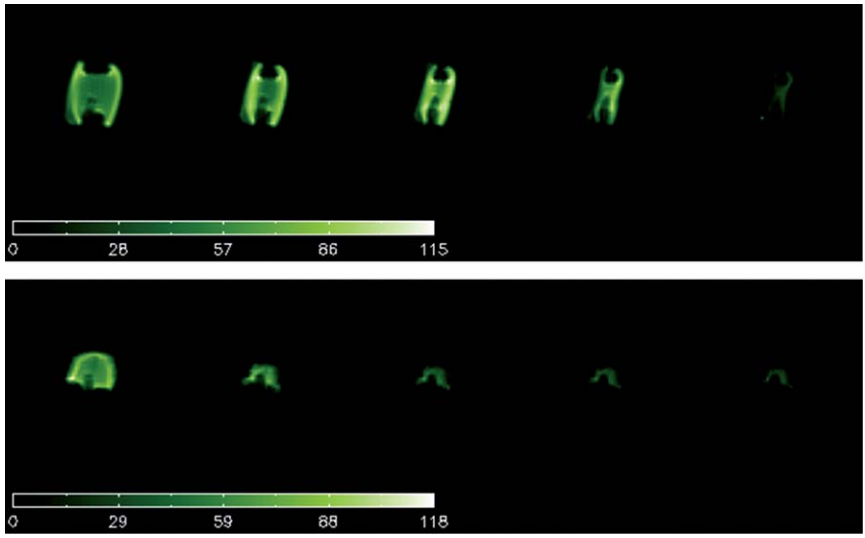

Fig. 8 MRI intensity of the middle slice of frozen broccoli stalks with respect to time. Samples are dried at 50 °C. Top: fresh sample frozen before drying. Bottom: sample first peeled then frozen before drying. Total drying time 4.5 hours.

It is also likely that the skin (cuticle) of fresh products forms a barrier for moisture transport, which amplifies the effects of the internal stress gradients. This leads to anisotropic shrinkage, and subsequent moisture transport towards the centre of product. Drying of fresh products no longer follows the standard Fick's law of diffusion. Drying models must be extended and the observed results show that stress-driven diffusion term must be included, similar to the work of Okozuno and Doi (2008).[18]

According to thermodynamics, it is even more proper to relate the moisture transport to gradients in chemical potential (or equivalently water activity or swelling pressure). If formulated in terms of the proper thermodynamic potential, there exists no anomaly. The formulation of transport in terms of gradients of thermodynamic potential is customary in the field of soft matter physics,[18,27] and food science can take advantage of this in adapting their framework.

Acknowledgements

This work is supported by the Energy Research Program EOS (EOS LT07043) of the Dutch Ministry of Economics.

References

1 K. P. Nott, L. D. Halla, J. R. Bows, M. Hale and M. L. Patrick, *Magn. Reson. Imaging*, 2000, **18**, 69–79.
2 A. LeBail, L. Boillereaux, A. Davenel, M. Hayert, T. Lucas and J. Y. Monteau, *Innovative Food Sci. Emerging Technol.*, 2003, **4**, 15–24.
3 X. Ye, R. Ruan, P. Chen and C. Doona, *LWT–Food Sci. Technol.*, 2004, **37**, 49–58.
4 K. Knoerzer, M. Regier, E. H. Hardy, H. P. Schuchmann and H. Schubert, *Innovative Food Sci. Emerging Technol.*, 2009, **10**, 537–544.
5 T. Lucas, D. Grenier, M. Bornert, S. Challois and S. Quellec, *Food Res. Int.*, 2010, **43**, 1041–1048.
6 M. Bouhrara, B. Lehallier, S. Clerjon, J.-L. Damez and J.-M. Bonny, *Magn. Reson. Imaging*, 2012, **30**, 422–430.
7 A. Mulet, N. Sanjuán, J. Bon and S. Simal, *Eur. Food Res. Technol.*, 1999, **210**, 80–83.

 This journal is © The Royal Society of Chemistry 2012

View Article Online

Published on 24 April 2012. Downloaded by Michigan State University on 25/01/2016 03:40:31.

8 P. N. T. Johnson, J. G. Brennan and F. Y. Addo-Yobo, *J. Food Eng.*, 1998, **37**, 233–242.
9 G. Arnaud and J. P. Fohr, *Int. J. Heat Mass Transfer*, 1988, **31**, 2517–2526.
10 F. Courtois, M. Abud Archila, C. Bonazzi, J. M. Meot and G. Trystram, *J. Food Eng.*, 2001, **49**, 303–309.
11 A. G. F. Stapley, T. M. Hyde, L. F. Gladden and P. J. Fryer, *Int. J. Food Sci. Technol.*, 1997, **32**, 355–375.
12 N. C. Reis, R. F. Griffiths, M. D. Mantle and L. F. Gladden, *Int. J. Heat Mass Transfer*, 2003, **46**, 1279–1292.
13 T. W. J. Scheenen, D. van Dusschoten, P. A. de Jager and H. Van As, *J. Magn. Reson.*, 2000, **142**, 207–215.
14 H. Watanabe, M. Fukuoka, A. Tomiya and T. Mihori, *J. Food Eng.*, 2001, **49**, 1–6.
15 K. W. Waldron, M. L. Parker and A. C. Smith, *Compr. Rev. Food Sci. Food Saf.*, 2003, **2**, 128–146.
16 S. Takeuchi, M. Maeda, Y.-i. Gomi, M. Fukuoka and H. Watanabe, *J. Food Eng.*, 1997, **33**, 281–297.
17 U. Wählby and C. Skjöldebrand, *J. Food Eng.*, 2001, **47**, 303–312.
18 T. Okuzono and M. Doi, *Phys. Rev. E: Stat., Nonlinear, Soft Matter Phys.*, 2008, **77**, 030501.
19 R. G. M. Van der Sman, *Food Hydrocolloids*, 2012, **27**, 529–535.
20 H. T. Edzes, D. van Dusschoten and H. Van As, *Magn. Reson. Imaging*, 1998, **16**, 185–196.
21 M. J. McCarthy, E. Perez and M. Ozilgen, *Biotechnol. Prog.*, 1991, **7**, 540–543.
22 R. G. M. Van der Sman, *Meat Sci.*, 2007, **76**, 730–738.
23 X. D. Chen, *Drying Technol.*, 2006, **24**, 121–122.
24 M. K. Krokida, Z. B. Maroulis and D. Marinos-Kouris, *Drying Technol.*, 1998, **16**, 687–703.
25 V. Y. Martínez, A. B. Nieto, P. E. Viollaz and S. M. Alzamora, *J. Food Sci.*, 2005, **70**, E12–E18.
26 B. Hiranvarachat, S. Devahastin and N. Chiewchan, *Food Bioprod. Process.*, 2011, **89**, 116–127.
27 M. Doi and A. Onuki, *J. Phys. II France*, 1992, **2**, 1631–1656.